Symmetry of Shapes Via Self-similarity

Xingwei Yang[1], Nagesh Adluru[1], Longin Jan Latecki[1],
Xiang Bai[2], and Zygmunt Pizlo[3]

[1] Temple University, Philadelphia
{xingwei,nagesh,latecki}@temple.edu
[2] Huazhong University of Science and Technology, Wuhan
xiang.bai@gmail.com
[3] Purdue University, West Lafayette
pizlo@psych.purdue.edu

Abstract. We describe a simple and novel approach to identify main similarity axes by maximizing self-similarity of object contour parts divided by the axes. For a symmetric or approximately symmetric shape, the main self-similarity axis coincides with the main axis of symmetry. However, the concept of the main self-similarity axis is more general, and significantly easier to compute. By identifying critical points on the contour self-similarity computation can be expressed as a discrete problem of finding two subsets of the critical points such that the two contour parts determined by the subsets are maximally similar. In other words, for each shape, we compute its division into two parts so that the parts are maximally similar. Our experimental results yield correctly placed maximal symmetry axes for articulated and highly distorted shapes.

1 Introduction

The idea of self-similarity of contours can be derived from the notion of good-continuation formulated by Gestalt Psychologists (Wertheimer [1]). Good continuation has usually been interpreted as representing smoothness of a contour, measured by a total curvature or curvature variation (e.g., Shaashua & Ullman [2]; Pizlo et al., [3].) However, examination of examples provided by Wertheimer [1] shows that good continuation was supposed to measure something more general than just curvature. Specifically, good continuation seemed to refer to symmetries of a contour: mirror, translational and rotational symmetry. In all these kinds of symmetry, one part of the contour is identical to another, except for translation, rotation or reflection transformations. For example, a sine wave has translational symmetry, whereas a square has mirror and rotational symmetries. But contours in a shape are almost never perfectly symmetric. Therefore, in order to find symmetry in a shape, instead of verifying identity of parts of contours, one should evaluate their *similarity*. It follows that a contour can be called approximately symmetric when it is self-similar. In particular, the conventional examples of good continuation, such as a straight line and a circle, are self similar. In contrast to the methods used for mathematically symmetric shapes, we

G. Bebis et al. (Eds.): ISVC 2008, Part II, LNCS 5359, pp. 561–570, 2008.

introduced a more general concept, which is an axis of self similarity. It also applies to non-rigid shapes, shapes with skewed symmetry, and performs well in the presence of contour noise.

It has been shown in Latecki & Lakamper [4] that a small set of critical points is sufficient to describe any planar shape in accord with human visual perception. Hence we measure self-similarity using a set of critical points on the contour. We employ the Discrete Curve Evolution method (DCE) ([4]) to compute the sets of critical points. Since the sets of critical points are very small (usually not exceeding 20 points) and since they capture all the information required for computing similarities, we are able to maximize self similarity by exhaustive search among axes of similarity. There have been many studies on shape similarity between objects based on their contours. In particular, Belongie, et al. [5] introduced shape context where shapes are represented using distance and angular histograms of the contour points and histogram-distance measures are used to obtain similarity between the shapes. They are also able to obtain correspondences between point sets on the two contours. Although they can obtain good results, they fail in the presence of articulations (deformations which are perception invariant), since they use Euclidean distance between points for distance histograms. In order to address this problem, Ling and Jacobs [6] replaced the Euclidean distance with geodesic distance, which is called inner distance and very related to skeleton matching [7]. The results of inner distance are, as expected, much better than shape context for articulated shapes. However, since they use tangent angles, the inner-distance is not stable in the presence of significant contour noise. Similar to [6], several approaches have been developed to address the problem of non-rigid shape matching and finding intrinsic symmetries, such as [8,9,10].

We introduce a shape representation and a shape similarity measure inspired by [6] and use it to compute main self-similarity axis. Since tangent angles are sensitive to contour noise, we use the histograms of only the geodesic distances between points. This has suitable properties for identifying self-similarities. The related work is briefly introduced in section 2. Section 3 describes the way we simplify the contour using critical points. The details of the self similarity maximization using geodesic distances are described in Sections 4 and 5. Finally, in Sections 6 experimental results are presented.

2 Related Work

The idea of using shape similarity to measure approximate symmetry is appealing, and has been proposed in the literature. Zabrodsky et al. [11], used contour shape similarity to detect symmetry. They explicitly apply each symmetry transformation to a given contour, for example 90° rotation, and then check whether the transformed contour and the original contour are similar. In the proposed approach, we do not explicitly compute any symmetry transformations but instead maximize self-similarity directly by subdividing the contour cleverly. This allows us to detect generalized symmetry axes as shown in Fig. 4, which are not detectable when applying mathematical symmetry transformations, e.g., rotations or mirror symmetry, to the input shapes. Geiger, et al. [12] also use contour similarity to find symmetry: They start with a 2D shape, its boundary contour, and two different parameterizations for the contour (one parametrization is oriented counterclockwise and the other clockwise). To measure its self-similarity, the two parameterizations are matched to derive the best set of one-to-one point-to-point correspondences along the contour. They use skeleton graphs to guide contour similarity computation, but the symmetry computation is still based on parameterized contour similarity. Many 3D objects in real world, man-made and natural, are bilaterally symmetric. Clearly, the symmetry is not perfect in the mathematical sense, but one could easily detect it if provided with good approximations of their surfaces [9,13]. Our goal is to recover symmetry from 2D shapes, but when 3D shapes projected onto a 2D space, the bilateral symmetry is generally distorted. Consider approximately planar surfaces of bilaterally symmetric 3D object that are themselves bilaterally symmetric. For such surfaces, assuming orthographic projection, viewed as an approximation to perspective projection, the shape contour exhibits skewed symmetry. The symmetry axis of the distorted shapes is the projection of the symmetry axis of the bilaterally symmetric planar surface of a 3D object. The symmetry axis and the skew angle make up two parameters that completely determine a skewed symmetry of a given planar object. The skew angle is the angle between the symmetry axis and parallel lines of symmetry that join corresponding symmetric points of the contour. Kanade [14] showed that the parameters of skewed symmetry constrain the possible orientations of the surface of the 3D object. This fact inspired a large amount of work on detecting skewed symmetry, e.g., Friedberg [15], Ponce [16]. However, these methods do not yield reliable results since they try to directly recover the parameters of skewed symmetry. In contrast, since our approach maximizes self-similarity we detect skewed symmetries without the need to recover the parameters. Also our self-similarity computation is far more general in that we can find partitions such that object parts have similar shapes. For examples see Fig. 4.

3 Extracting Critical Points Using DCE

The Discrete Curve Evolution (DCE) method was introduced in [4]. Contours of objects (shapes) in digital images are distorted by digitization noise and segmentation errors. Hence it is desirable to eliminate the distortions while at the same time preserve the perceptual appearances sufficient for object recognition. DCE accomplishes this goal by treating the contour as a polygon and recursively removing least relevant vertices according to a well-motivated measure. This process is illustrated in Fig. 1, where the red lines illustrate the simplified polygons. In each evolutional step, a pair of consecutive line segments S_1, S_2 is replaced by a single line segment joining the endpoints of $S_1 \cup S_2$. The key

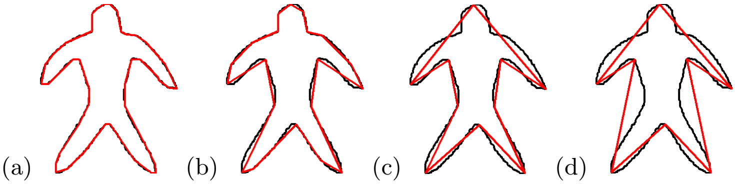

Fig. 1. The evolution of the Discrete Curve Evolution. The red lines are simplified polygons and the blue lines are the original contours. From (a) to (d), the polygons become more and more simple.

property of this evolution is the order of the substitution. The substitution is achieved according to relevance measure K given by:

$$K(S_1, S_2) = \frac{\beta(S_1, S_2) l(S_1) l(S_2)}{l(S_1) + l(S_2)} \tag{1}$$

where line segments S_1, S_2 are the sides of the polygon incident at a vertex $v, \beta(S_1, S_2)$ is the turn angle at the common vertex of segments S_1, S_2, and l is the length function normalized with respect to the total length of a polygonal curve C. The main property of this relevance measure is explained in [4]. The higher the value of $K(S_1, S_2)$, the larger is the contribution of the arc $S_1 \cup S_2$ to the shape. Therefore, the process eliminates the less important points while keeping the important points. In our approach, we obtain contour divisions using the set of critical points given by the vertices of the DCE simplified polygon.

4 Maximizing Self-similarity

The intuition is that we divide a given shape into two parts, and compute their dissimilarity value. The parts that minimize the dissimilarity value, i.e., maximize self-similarity, are used to define a main similarity axis, which for many shapes corresponds to the main axis of symmetry. Clearly, for simple geometric objects like a ball, the main axis of symmetry (as well as the main similarity axis) is not defined, since it is not unique. However, for most shapes it is unique, and the proposed approach is able to determine the main axis of symmetry. Also some objects exhibit more than one axis of symmetry (e.g., the letter x). The proposed approach can be easily extended to handle such cases. For simplicity of presentation we describe the computation of a unique, main similarity axis.

The shape is divided into pairs of sub-parts using the critical points obtained by Discrete Curve Evolution. For a given shape, let $V = (v_1, \ldots, v_M)$ be the critical points. We assume a clockwise direction of contour traversal. Any two indices $i, j \in \{1, \ldots, M\}$ such that $i + 1 < j (mod\ M)$ and $j + 1 < i (mod\ M)$ define four divisions into two possibly overlapping subsequences of V with the cyclic order $mod\ M$:

1. $(v_i, \ldots, v_j), (v_{j+1}, \ldots, v_{i-1})$; 2. $(v_i, \ldots, v_j), (v_j, v_{j+1}, \ldots, v_{i-1}, v_i)$
3. $(v_i, \ldots, v_j), (v_j, v_{j+1}, \ldots, v_{i-1})$; 4. $(v_i, \ldots, v_j), (v_{j+1}, \ldots, v_{i-1}, v_i)$

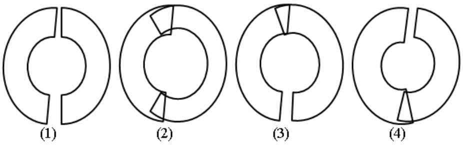

Fig. 2. Pictorial illustration of the four divisions: (1) No common endpoint. (2) Two common endpoints. (3) and (4) One common endpoint.

A pictorial illustration of the four divisions is shown in Fig. 2.

Any of the four sequence divisions determines a shape division into two (possibly overlapping) contour segments relative to the two endpoints v_i, v_j. (Two ends of the contour segments can overlap only in one critical point.) For example, let us consider the convex critical endpoint pair 1, 3 in Fig. 3(a). It determines the following sequence divisions, and their corresponding sub-contours:

$$(1)\ (1,2,3),(4,5);(2)(1,2,3),(3,4,5,1);\ (3)\ (1,2,3),(3,4,5);(4)(1,2,3),(4,5,1)$$

Two simplified sub-contours which are induced by sequence division (4) are shown in Fig. 3(b).

For a given sequence division $(v_i,\ldots,v_j)$, $(v_{j+1},\ldots,v_{i-1})$, (we consider division pair (1) first), we define an induced division of the contour G into two possibly overlapping sub-contours S and T. The sub-contour S is defined as the union of critical points $(v_i,\ldots,v_j)$. Similarly, we define the sub-contour T with respect to $(v_{j+1},\ldots,v_{i-1})$. Observe that the corresponding sequences are exactly the vertices of S and T. While the order of endpoints in S is determined by the first sequence order, the order of endpoints in T is determined by the second sequence in reversed order. This means that the critical points $(v_i,\ldots,v_j)$ of S are traversed clockwise while the critical points $(v_{j+1},\ldots,v_{i-1})$ of T are traversed counterclockwise. The same definition of the pair of sub-contours S and T applies to division pairs (2), (3), and (4).

Given a pair of induced sub-contours S, T, we compute their dissimilarity $c(S,T)$, where c is defined in Section 5, below. By enumerating all valid pairs of critical points indices $i,j \in \{1,\ldots,M\}$ and the four possible sub-contours for

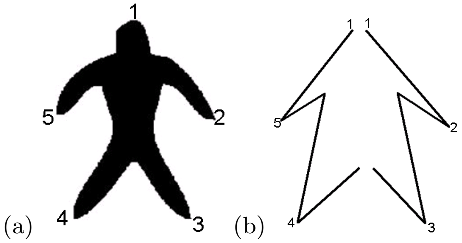

Fig. 3. (a) The contour endpoints. (b) The sub-contour division induced by endpoint sequence division (1,2,3), (4,5,1).

each index pair, we find a pair of sub-contours S, T with the minimal dissimilarity $c(S, T)$. The obtained sub-contour division then defines the main self similarity axis. For symmetric and nearly symmetric shapes, the main self similarity axis corresponds to the main axis of symmetry.

Observe that the proposed approach is guaranteed to find the global minimum of self similarity of the contour of every planar shape, since we maximize the self similarity in the discrete domain determined by the index pairs. Also the number of dissimilarity comparisons needed is $O(M^2)$. Usually M is a very small number: even for complex shapes it is typically not larger than 20.

Since we do not know the optimal number of DCE vertices to best represent a given shape, we generate a range of 16 possible representation levels from coarse (5 vertices) to fine (20 vertices). At each representation level we find the self-similarity axis as explained above. The final symmetry axis is the best self-similarity axis chosen from across the 16 levels.

5 Self-similarity Measure

Each division constructed in the previous section produces a pair of sub-segments of a given contour. In this section we explain the similarity measure used to compare two sub-segments of the contour. Our similarity measure is motivated by inner distance introduced in [6]. The advantage of geodesic distance is that it is insensitive to the articulation of parts, which is very important for shape similarity. Compared to geodesic distance, the Euclidean distance does not have this property. The reason for this is the Euclidean distance does not consider whether the line segment crosses shape boundaries. Based on the above discussion, even though the shape itself is distorted, the inner-distance descriptor is able to represent the shape correctly. Therefore, the proposed method uses inner-distance instead of Euclidean distance. However, since the proposed approach is for obtaining symmetric division within the same shape, we adapt it so as to be more suitable for measuring *self-similarity* of shapes. For each sub-part we compute a vector of geodesic distances between the contour points in that part. The order is determined using critical points that actually induce divisions. The reasons for discarding the angular information are (1) it is sensitive to contour noise and (2) it is not so discriminative for symmetry based on self-similarity. Observe that we use vectors of geodesic distances instead of distance histograms. Instead of computing the vectors for each division separately, we first compute the distances and store them. We keep the order of points in two directions (clockwise and counter clockwise) when we calculate the geodesic distance from the current point to all other points. Therefore, for a shape which has N sample points $\{x_1, x_2, \ldots, x_{N-1}, x_N\}$ and $M << N$ critical points $\{v_1, v_2, \ldots, v_{M-1}, v_M\}$ chosen from the N sample points using DCE, there will be two distance matrices, for clock-wise and counter clockwise directions. For each critical point v_i, the clockwise distance vector to all N sample points is given by:

$$D(v_i) =< d(v_i, x_k), d(v_i, x_{k+1}), \ldots, d(v_i, x_{k+N-2}), d(v_i, x_{k+N-1}) > \qquad (2)$$

where, x_k is the closest sample point to v_i and $k + m = (k + m \mod N)$ and $d(v_i, x_k)$ is the value of geodesic distance between the points v_i and x_k.

The counter-clockwise distance vector of v_i is given by flipping the sequences in eq. (2):

$$D'(v_i) =< d(v_i, x_{k+N-1}), d(v_i, x_{k+N-2}), \ldots, d(v_i, x_{k+1}), d(v_i, x_k) > \tag{3}$$

The proposed method has three main steps for the shape similarity. First for two vertices v_i and v_j, which are from different sets, the distance between them is calculated by

$$c(v_i, v_j) = \|D(v_i) - D'(v_j)\| \tag{4}$$

Then for two different sub-contours S and T (Section 4), with critical points $[v_i]_{i=1}^{M_1}$ in clockwise direction and $[v_j]_{j=1}^{M_2}$ in counter clockwise direction, we compute all distances between the points by formula (4) and obtain a distance matrix:

$$c(S,T) = \begin{bmatrix} c(v_1, v_1') & c(v_1, v_2') & \cdots & c(v_1, v_{M_1}') \\ c(v_2, v_1') & c(v_2, v_2') & \cdots & c(v_2, v_{M_1}') \\ \vdots & \vdots & \ddots & \vdots \\ c(v_{M_1}, v_1') & c(v_{M_1}, v_2') & \cdots & c(v_{M_1}, v_{M_1}') \end{bmatrix}$$

Finally we compute the distance $c(S,T)$ between sub-contours S and T as the shortest path in matrix $C(S,T)$ from $c(v_1, v_1')$ to $c(v_{M_1}, v_{M_1}')$ using dynamic programming [17]. It is equivalent to computing the dissimilarity value $c(S,T)$ by the optimal matching of the critical points from S to T with dynamic time warping.

6 Experimental Results

In this section we present the results of the described approach on a set of shapes from (Aslan and Tari [18]). In [18], the authors introduced a shape matching algorithm based on the skeleton of shape. Though the method can obtain excellent results for shape similarity, it seems hard to extend it for self-similarity. The dataset exhibits large shape variance due to distortion and articulation within each class, composed of four shapes. The results in Fig. 4 demonstrate that the proposed method is stable for articulated shapes. The red lines and blue lines represent two different shape symmetric sub-contours for each shape. Observe that the proposed method can obtain correct shape symmetric sub-contours for articulated shapes and it is also stable for obviously symmetric shapes as shown in Fig. 4. Moreover, the results in Fig. 5 show that even if the shape is not naturally symmetric, the proposed method can find a shape-symmetric division into two sub-contours which corresponds to a human's intuition. For example, the head of the horse is symmetric to tail and the two front legs are symmetric to the two rear legs. We demonstrated that the proposed method is robust for calculating the symmetric division of articulated and distorted shapes. Now we show that it is also useful for determining skewed symmetry, which is very

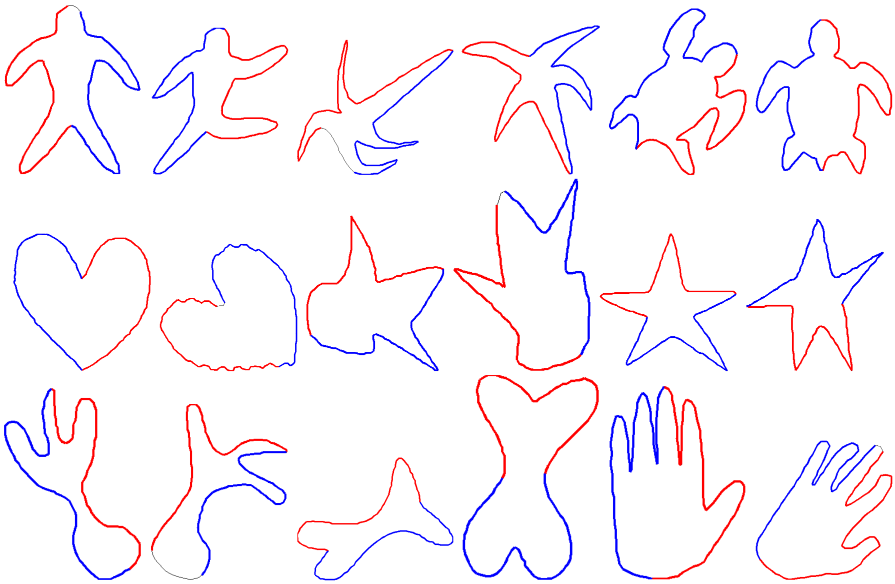

Fig. 4. The symmetric results for articulated objects, The red lines and blue lines represent the symmetric sets. The gray lines are the lines which are skipped by the proposed method.

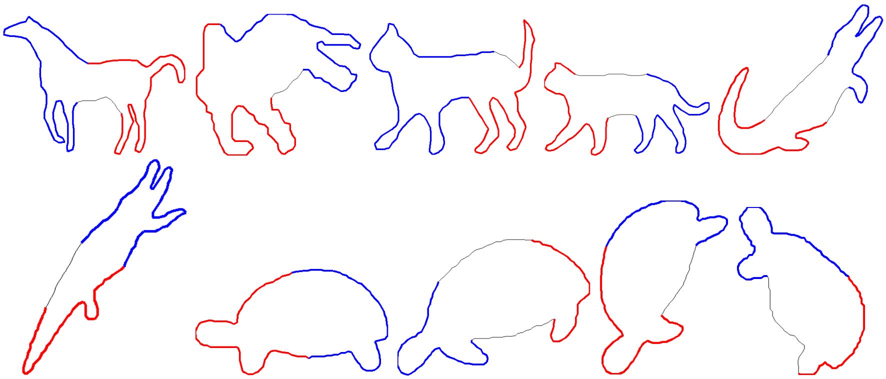

Fig. 5. The symmetric results for objects which are not naturally symmetric. The red lines and blue lines represent the symmetric sets. The gray lines are the lines which are skipped by the proposed method.

important for detection of 3D mirror symmetry. As stated in Section 2, the symmetry axis of the skewed symmetry is the orthographic projection of the symmetry axis of the bilaterally symmetric planar surface of a 3D object. We illustrate in Fig. 6 that the proposed method can be used to recover the main axis of skewed symmetry. Certainly, if the shape is too skewed, the proposed

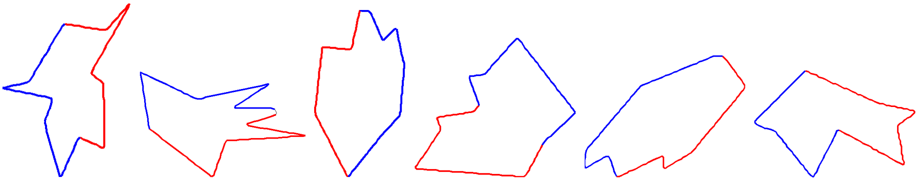

Fig. 6. The symmetry results on skewed symmetric shapes. The red lines and blue lines represent the symmetric sets. The gray lines are the lines which are skipped by the proposed method.

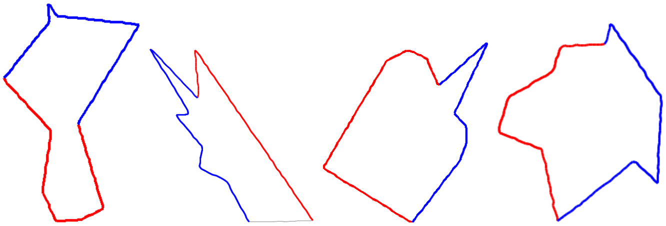

Fig. 7. The wrong symmetry results in the presence of strongly skewed symmetric shapes. The red lines and blue lines represent the symmetric sets. The gray lines are the lines which are skipped by the proposed method.

method cannot find the correct symmetric division. For example, the results in Fig. 7 show some incorrect divisions. However, examination of the shapes in Fig. 7, suggests that even humans may have problems identifying the axis of skewed symmetry.

7 Conclusions

We proposed a simple and novel method for computing symmetry of a shape that yields results in accordance with human intuition. We use vectors of geodesic distances to exploit the order of contour points for self-similarity. The experimental results show that the proposed method obtains correct shape symmetry division not only for articulated shapes, but also for skewed symmetric shapes, which is very important in determining the symmetry of 3D objects.

Acknowledgments

We thank Tadamasa Sawada for providing the dataset used for identifying the axis of skewed symmetry. This work was supported in part by the NSF Grants IIS-0534929, IIS-0812118, and by the DOE Grant DE-FG52-06NA27508.

References

1. Werthimer, M.: Principles of perceptual organization. In: Beardslee, D.C., Wertheimer, M. (eds.) Readings in Perception, pp. 115–135 (1923/1958)
2. Shaashua, A., Ullman, S.: Structual saliency: the detection of global salient structures using a locally connected network. In: ICCV, pp. 321–327 (1988)
3. Pizlo, Z., Salach-Colyska, M., Rosenfeld, A.: Curve detection in a noisy image. Vision Research 37, 1217–1241 (1997)
4. Latecki, L.J., Lakamper, R.: Convexity rule for shape decomposition based on discrete contour evolution. CVIU 73, 441–454 (1999)
5. Belongie, S., Malik, J., Puzicha, J.: Shape matching and object recognition using shape context. IEEE Trans. PAMI 24, 509–522 (2002)
6. Ling, H., Jacobs, D.W.: Shape classification using inner-distance. IEEE Trans. PAMI 29, 286–299 (2007)
7. Bai, X., Latecki, L.J.: Path similarity skeleton graph matching. IEEE Trans. PAMI 30, 1282–1292 (2008)
8. Bronstein, A.M., Bronstein, M.M., Bruchstein, A.M., Kimmel, R.: Matching two-dimentional articulated shapes using generalized multidimentional scaling. In: Proc. Conf. on Articulated Motion and Deformable Objects, pp. 48–57 (2006)
9. Bronstein, A.M., Bronstein, M.M., Kimmel, R.: Rock, paper, and scissors: extrinsic vs. intrinsic similarity of non-rigid shapes. In: ICCV (2007)
10. Bronstein, A.M., Bronstein, M.M., Kimmel, R.: Analysis of two-dimentaional non-rigid shapes. IJCV 78, 67–88 (2008)
11. Zabrodsky, H., Peleg, S., Avnir, D.: A measure of symmetry based on shape similarity. In: CVPR, pp. 703–706 (1992)
12. Geiger, D., Liu, T., Kohn, R.V.: Representation and self-similarity of shapes. IEEE Trans. PAMI 25, 86–100 (2003)
13. Raviv, D., Bronstein, A.M., Bronstein, M.M., Kimmel, R.: Symmetries of non-rigid shapes. In: Proc. Workshop on Non-rigid Registration and Tracking through Learning (2007)
14. Kanade, T.: Recovery of the three-dimensional shape of an object from a single view. Artificial Intelligence 17, 409–460 (1981)
15. Friedberg, S.A.: Finding axes of skewed symmetry. CVGIP 34, 138–155 (1986)
16. Ponce, J.: On characterizing ribbons and finding skewed symmetries. CVGIP 52, 328–340 (1990)
17. Cormen, T.H., Leiserson, C.E., Rivest, R.L., Stein, C.: Introduction to algorithms, 2nd edn. MIT Press, Cambridge (2001)
18. Aslan, C., Tari, S.: An axis based representation for recognition. In: ICCV, pp. 1339–1346 (2005)